

Cryogenic R5912-20Mod Photomultiplier Tubes Characterization for the ProtoDUNE Dual Phase Experiment

D. Belver,^a E. Calvo,^a C. Cuesta^{a,1} A. Gallego-Ros,^a I. Gil-Botella,^a S. Jiménez,^a
C. Lastoria,^a T. Lux,^b C. Palomares,^a D. Redondo,^a F. Sanchez,^b J. Soto-Oton,^a A. Verdugo,^a

^a*Centro de Investigaciones Energéticas, Medioambientales y Tecnológicas (CIEMAT), Av Complutense 40, 28040, Madrid, Spain*

^b*Física d'Altes Energies (IFAE) - The Barcelona Institute of Science and Technology, Campus UAB, Bellaterra (Barcelona), Spain*

E-mail: clara.cuesta@ciemat.es

ABSTRACT: The Deep Underground Neutrino Experiment (DUNE) is a dual-site experiment for long-baseline neutrino oscillation studies, and for neutrino astrophysics and nucleon decay searches. The far detector is a 40-kton underground liquid argon time-projection-chamber (LAr TPC), in which the photon detector system adds precise timing capabilities. The ProtoDUNE dual phase detector will consist of a $6\times 6\times 6\text{ m}^3$ LAr TPC to be operated at the CERN Neutrino Platform and the photon detection system will be formed by 8-inch cryogenic photomultipliers from Hamamatsu. The validation measurements of the PMT model (R5912-20Mod) and the base design at cryogenic temperatures are described. Also, the characterization results of the 40 photomultipliers to be used in ProtoDUNE dual phase are presented.

KEYWORDS: Noble liquid detectors (double-phase); photon detectors (photomultipliers); neutrino detectors;

¹Corresponding author.

Contents

1	Introduction	1
2	PMT unit	3
3	Testing set-up	5
4	PMT measurements methodology	6
4.1	Dark Current	7
4.2	Gain and fatigue effect	7
4.3	Linearity	9
4.4	Light rate	9
5	PMT validation results	11
5.1	Dark Current	11
5.2	Gain	12
5.3	Linearity	12
5.4	Light rate	13
5.5	PMT base validation	15
6	ProtoDUNE-DP PMT characterization	15
6.1	Dark Current	16
6.2	Gain	16
	Conclusions	17

1 Introduction

The DUNE experiment aims to address key questions in neutrino physics and astroparticle physics [1]. It includes precision measurements of the parameters that govern neutrino oscillations with the goal of measuring the CP violating phase and the neutrino mass ordering, nucleon decay searches, and detection and measurement of the electron neutrino flux from a core-collapse supernova within our galaxy. DUNE will consist of a near detector placed at Fermilab close to the production point of the muon neutrino beam of the Long-Baseline Neutrino Facility (LBNF), and four 10 kt fiducial mass LAr TPCs as far detector in the Sanford Underground Research Facility (SURF) at 4300 m.w.e. depth at 1300 km from Fermilab [2].

In order to gain experience in building and operating such large-scale LAr detectors, an R&D programme is currently underway at the CERN Neutrino Platform [3]. Such programme will operate two prototypes with the specific aim of testing the design, assembly, and installation procedures, the detectors operations, as well as data acquisition, storage, processing, and analysis. The two

prototypes will employ LAr TPCs as detection technology. One prototype will only use LAr, called ProtoDUNE Single-Phase, and the other will use argon in both its gaseous and liquid state, thus the name ProtoDUNE Dual-Phase (DP). Both detectors will have similar sizes. In particular, ProtoDUNE-DP [4], also known as WA105 (NP02), will have an active volume of $6 \times 6 \times 6 \text{ m}^3$ corresponding to a mass of 300 t. A schematic drawing of ProtoDUNE-DP is shown in Figure 1. In ProtoDUNE-DP the charge is extracted, amplified, and detected in gaseous argon above the liquid surface allowing a finer readout pitch, a lower energy threshold, and better pattern reconstruction of the events.

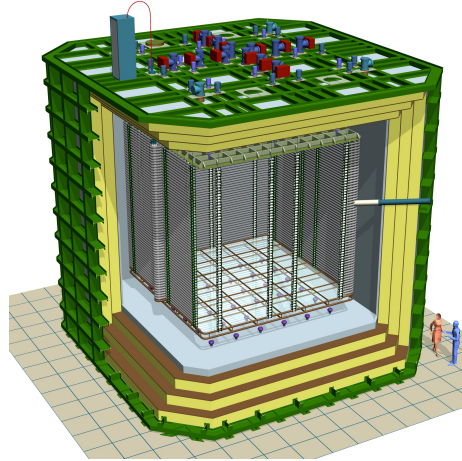


Figure 1. Schematic drawing of ProtoDUNE-DP where the 36 PMTs are installed at the bottom of the active volume.

In the case of a charged particle traversing the LAr, the medium is ionized and at the same time photons of 128 nm are emitted. The scintillation light signal is used as trigger for non-beam events, to determine precisely the event time, for cosmic background rejection, and there is also a possibility to perform calorimetric measurements and particle identification. The prompt scintillation light (usually referred as S1 signal) in LAr has two components: S1 fast of $\sim 6 \text{ ns}$, and S1 slow of $\sim 1.6 \mu\text{s}$. In addition, the electroluminescence, secondary scintillation light called S2, is produced in the gas phase of the detector when electrons, extracted from the liquid, are accelerated in the electric field between the liquid phase and the anode. The time stretch of S2 reflects the maximum drift time of original ionization in the liquid phase up to the gas phase, thus for $\sim 1 \text{ kV/cm}$ electric field, the time scale of S2 is of the order of hundreds of microseconds

The photon detection system of ProtoDUNE-DP [5] is formed by 36 8-inch cryogenic photo-multipliers (PMTs) placed at the bottom of the active volume, behind the highly transparent cathode. As wavelength-shifter, tetraphenyl butadiene (TPB) is coated directly on the PMTs. The photon detection system must have precision timing capabilities of few ns, a wide dynamic range to record from a few photo-electrons (p.e.) to thousands of p.e., a linear response even under high frequency or high intensity light conditions, and be able to operate at cryogenic temperature.

This paper describes the PMT and base circuit to be used in ProtoDUNE-DP in section 2. The dedicated facility used to carry out the PMT studies is presented in section 3. Section 4 introduces the approach and procedure used in the measurements. The PMT validation measurements are

detailed in section 5, and the characterization results of the 36 PMTs to be used in ProtoDUNE-DP are described in section 6. Finally, the results of the PMT performance at cryogenic temperatures that can be valuable for other experiments are summarized in the conclusions.

2 PMT unit

The photon detection system of the ProtoDUNE-DP experiment is based on Hamamatsu R5912-20Mod cryogenic photomultipliers [6]. This 8-inch diameter PMT was selected as the light sensor since a large sensor coverage of the cathode area of 36 m^2 should be achieved and also due to its proven reliability on other cryogenic detectors. The same or similar PMTs were successfully operated in other LAr experiments like MicroBooNE [7], MiniCLEAN [8], ArDM [9] and ICARUS T600 [10].

These devices can operate at a gain up to 10^9 at room temperature (RT), required to compensate the gain loss at cryogenic temperatures (CT). The high number of dynodes also has the advantage of requiring a lower operation voltage for a given gain compared with PMTs with lower number of dynodes, which reduces the potential risk of sparks and the heat dissipation in the PMT bases. As the PMTs are designed to operate at low cryogenic temperatures, a thin platinum layer was added between the bi-alkali photo-cathode and the borosilicate glass envelope to preserve the conductivity of the photocathode at these temperatures. The cathode sensitivity provides a spectral response from 300 to 650 nm. It is worth noting that the PMT tests described in this paper are done prior to the TPB coating.

An individual PMT support structure was designed, manufactured and assembled at CIEMAT. This structure is mainly composed of 304L stainless steel with some small Teflon (PTFE) 6.6 pieces assembled by A4 stainless steel screws that minimize the mass while ensuring the PMT support to the cryostat membrane. The design takes into account the shrinking of the different materials during the cooling process to avoid the break of the PMT glass. The PMTs are placed at the bottom of the ProtoDUNE-DP membrane fixed to an stainless steel plate which is glued to the membrane. A picture of one PMT assembled on its support is shown in Figure 2.



Figure 2. Picture of R5912-20Mod PMT with the mechanical support, the PMT base, and its cable.

The PMT base was designed with passive components due to bad working of semiconductors on cryogenic conditions. The components were carefully selected and tested in order to minimize their variations with the temperature. The circuit resistors were chosen following the voltage ratio recommended by the manufacturer to increase the linearity range on the space-charge effect area. The total resistance of the circuit was set to 13.4 M Ω with an average current $\sim 100 \mu\text{A}$ (depending on the required voltage for each PMT), and the power dissipated per PMT base $\sim 0.14 \text{ W}$.

In order to choose the optimal PMT base design for ProtoDUNE-DP, two possible voltage configurations (positive and negative bias) were considered (see Figure 3). In the so called positive base (PB) [7], a positive high voltage (HV) is applied at the anode and the photocathode is grounded, which reduces the noise; whereas in the negative base (NB) [10, 11], a negative HV is applied at the cathode and the anode is grounded. In the negative bias configuration, the photocathode is connected to HV, and special care must be taken to prevent spurious pulses due to HV leakage through the glass tube envelope to nearby grounded structures. The NB configuration requires two cables, one for HV and the other for the signal readout. Nevertheless, in this configuration it is easier to read the PMT signal as it is referenced to ground. On the other hand, one advantage of the PB is that only one coaxial cable is required to carry the positive HV and to receive the signal from the PMT, but a decoupling circuit is needed to split the HV and the PMT signal. A dedicated splitter circuit was designed at CIEMAT to perform this function out of the cryostat. The splitter affects the real voltage value that is sent to the PB which is expected to be a $\sim 7\%$ lower than the one read on the power supply. After some validation measurements, see section 5.5, the PB design was selected for ProtoDUNE-DP, as the total number of cables and feedthroughs in the detector is reduced and its behavior in terms of linearity and dark current is slightly better than the NB. All results presented in this study were achieved using the PB design with the exception of the results discussed in section 5.5.

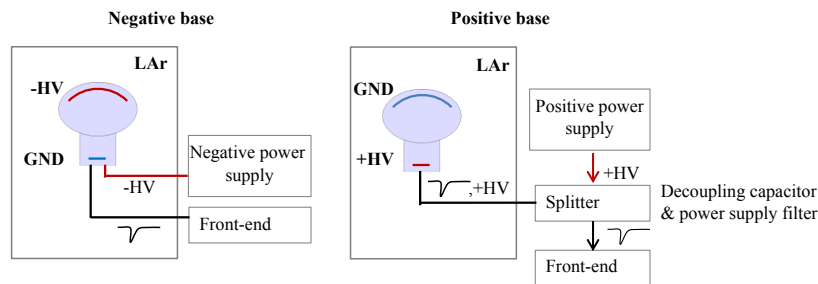


Figure 3. Schematic drawing of the two HV divider options for the base.

Once the PB was selected, all the bases were assembled, cleaned and tested at CIEMAT in air, Ar gas and liquid nitrogen (LN_2). Two tests were performed to the bases before being soldered to the PMTs and tested at CT: a resistance value of $13.4 \pm 0.1 \text{ M}\Omega$ was confirmed, and 2000 V were applied to the bases in Ar gas to verify the absence of sparks.

3 Testing set-up

A dedicated test bench was designed at CIEMAT for the PMT characterization. The measurements are performed to 10 PMTs at the same time inside a 300 L vessel at RT and filled with LN₂ at 77 K for the CT tests. A schematic drawing is shown in Figure 4. The vessel set-up and 10 PMTs installed are shown in Figure 5.

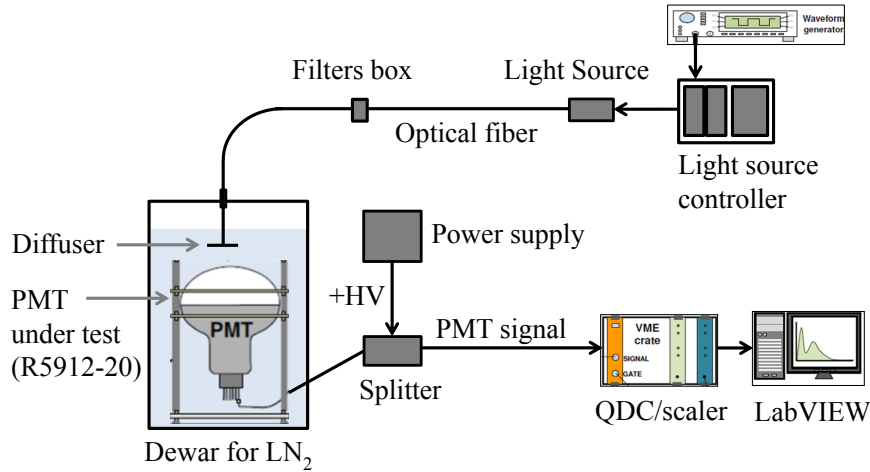


Figure 4. Schematic drawing of the PMT testing experimental set-up.

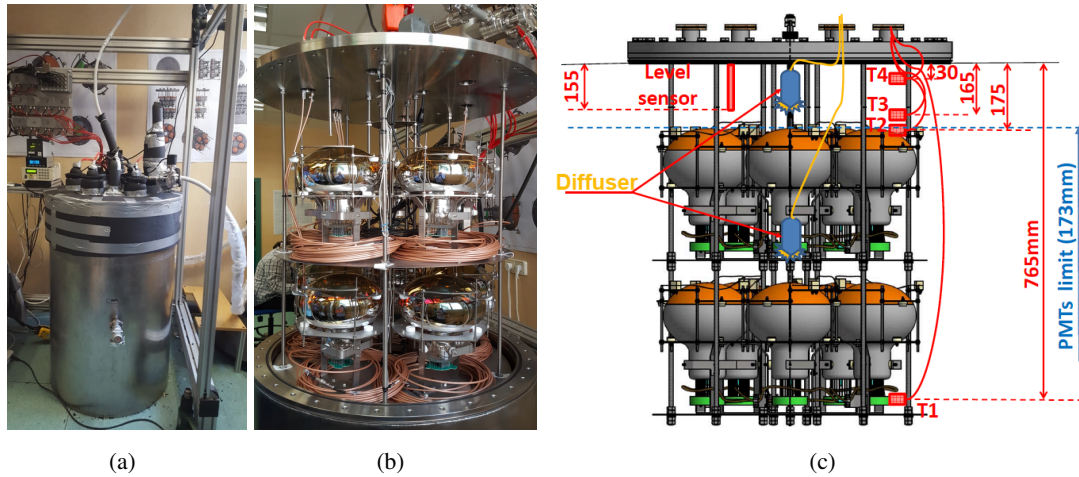


Figure 5. (a) 300 L vessel used in the testing set-up. (b) 10 PMTs being installed in the vessel. (c) Schematic drawing showing the distribution of the 10 PMTs, temperature sensors (T1-T4), diffusers, and level sensor inside the vessel.

A 400 L tank supplies LN₂ at ~2 atm pressure through a pipe directly to the 300 L vessel where the PMTs are located at ambient pressure. A diagram of this system is shown in Figure 6. The system is automatically filled, using electro-valves controlled by level probes and temperature probes through a PC. The 10 PMTs are distributed in two levels, five per level, fixed to the lid through

an internal structure, see Figure 5(c). The cables of the PMTs, temperature and level sensors, and optical fibers pass through several CF40 ports. Each PMT is fixed to the internal structure with two M6 screws using the same support as it will be done in ProtoDUNE-DP. The PMTs are connected to the vessel feed-through by means of the same 21 m cable that will be used on the final installation. The opening and closing of the lid is carried out with a little crane.

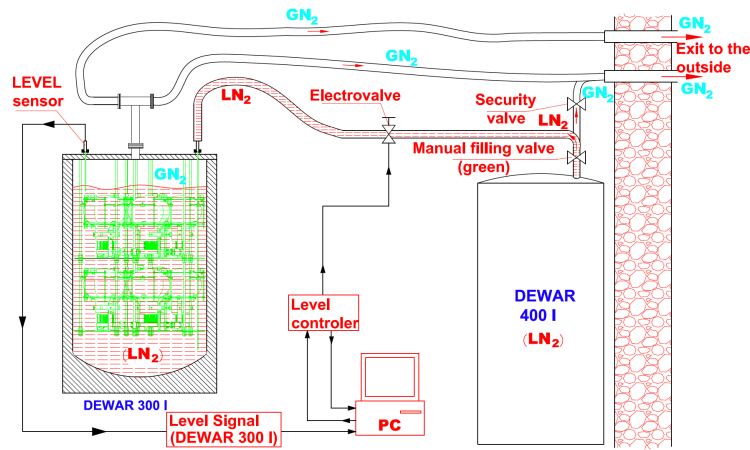


Figure 6. Detailed cryogenics set-up for 10 PMT testing.

The main PMT features to measure are dark current, gain, and linearity. For each feature, a different electronics set-up is arranged. To perform the dark current acquisition, a V895 discriminator and a V560E scaler tandem from CAEN¹ is used. In order to calculate the gain and study the PMT response to light, the PMT output is measured with a V965A CAEN Charge-to-Digital Converter (QDC). The PMTs are biased using CAEN's N1470 power supply. The DAQ is remotely controlled with the aim of automating the data acquisition with LabVIEW software².

The light sources used are a PicoQuant GmbH³ laser head, with a 405 nm wavelength and a pulse width less than 500 ps FWHM, and an LED pulser, with a 460 nm wavelength and a pulse width of 40 ns FWHM. The QDC integration window and the light source are synchronized using a two output signal generator. The light is driven inside the dewar using hard clad silica multimode optical fibers from Thorlabs⁴. The amount of light is tuned using a set of UV optical filters and the light is diffused in the detector volume.

4 PMT measurements methodology

In this section, the approach and procedures used in the measurements, and the expected results are detailed. The studies carried out to fully understand the PMT behavior at CT include the dark current, the gain, and the linearity.

¹<http://www.caen.it/>

²<http://www.ni.com/>

³<https://www.picoquant.com/>

⁴<https://www.thorlabs.com/>

4.1 Dark Current

The dark current (DC) rate is the response of the PMT in absence of light. It is known that the main contribution to the DC at RT is the thermionic emission [12]. However, a non-thermal contribution increases the DC rate at CT [13, 14]. The DC rate is estimated as the average rate of detected signals larger than 7 mV, which assures SPE triggering at an operating gain of 10^7 in a completely dark state. At RT, measurements were taken after at least 15 hours of complete darkness inside the vessel. The DC evolution with time right after immersing the PMTs in LN₂ and closing the vessel is shown in Figure 7. It is clearly observed that initially the DC rate drops by more than one order of magnitude as the PMT was exposed to ambient light before the measurement. Then, the DC rate comes to a stable value with a small increase. As the PMT needs time to stabilize, DC measurements at CT were taken after ~ 3 days. The same behavior is observed for all the tested PMTs.

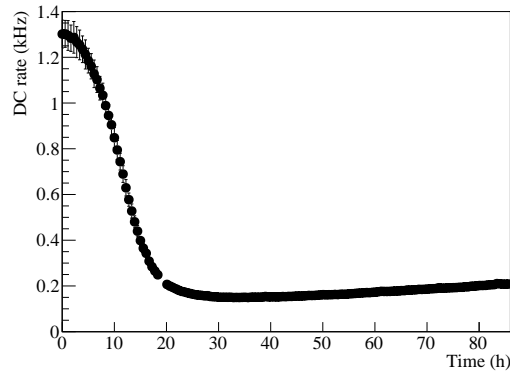


Figure 7. Evolution of the DC rate when cooling down a PMT. DC measurements are taken every 10 s and averaged every 13 min in the plot (error bars are the rms).

The DC as a function of the HV is measured in 100 V steps from 1000 V to 1900 V at RT and CT. Additionally, as the PMT manufacturer provided a reference value of the DC rate for every PMT at a gain of 10^9 at RT, a similar measurement of the DC at that gain is also performed. The conditions defined by Hamamatsu to measure the DC rate differ from the ones explained above, as the trigger is made at SPE level for a 10^9 gain, which is a higher threshold than the one used at CIEMAT.

4.2 Gain and fatigue effect

To characterise the gain of each PMT, a small amount of photons is sent to the PMT to obtain the SPE spectrum. The SPE spectrum is fitted to a convolution of a Poisson distribution, which models the number of p.e. generated in the photocathode, and a binomial distribution considering two possible amplification paths: through the first dynode and directly starting in the second dynode [15]. An example of the fit is shown in Figure 8.

The gain vs HV, known as gain calibration curve, is measured from 1100 V to 1900 V in 100 V steps. Then, a fit is done following the power law $G = AV^B$ being A and B constants dependent on the number, structure, and material of the dynodes.

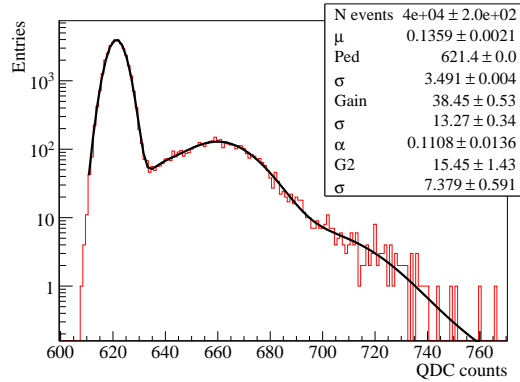


Figure 8. SPE spectrum (red) of a PMT at CT at 1500 V, and fit results (black) where μ is the mean number of p.e. Ped the position of the pedestal, $Gain$ is the gain of a p.e., in QDC counts, generated in the photocathode when it is amplified from the first dynode, $G2$ from the second dynode, and α is the proportion of p.e. amplified by the second dynode.

The gain evolution with time right after immersing the PMTs in LN_2 is shown in Figure 9. During the first ~ 5 hours the gain increases as the PMT vacuum improves, then it drops during ~ 10 hours by a factor of 4 while the PMT is cooling down. Finally, a small drift takes place and gain reaches a stable value after ~ 3 days. As a result, tests are taken always at least 3 days after immersion. A very similar behavior is reported in [7].

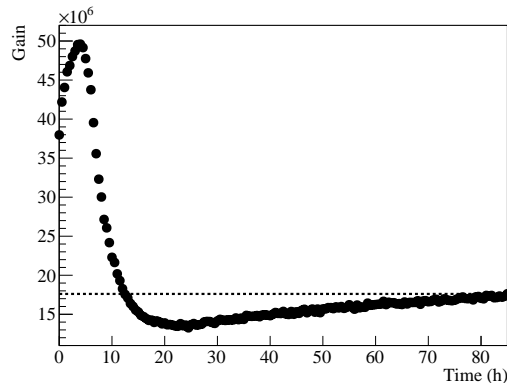


Figure 9. Evolution of the gain when cooling down a PMT. Gain is calculated every 30 minutes. The dotted line represents the nominal gain obtained 3 days after immersing the PMTs in LN_2 .

A variation of the gain is expected when the PMT output current increases, either, due to high gain, to high light intensity or to high rate of the light (or a combination of them). This variation of the gain is called fatigue [16] and can distort the results of the measurements if the PMT cannot recover from this effect between measurements. At RT, no variation of the PMT gain is observed during the tests. For some reason, the PMT fatigue recovery is much slower at CT allowing to observe a gain reduction. This gain reduction depends on the PMT output current generated during the previous test. In addition, once the cause of the gain reduction is over, the PMT requires a long time to recover the initial gain, and this time is also dependent on the amount of current generated

in the PMT. Both factors, gain reduction and recovery time, vary from one PMT to another.

The PMT gain is monitored over time after the tests that produce a high PMT output current. The gain monitoring is performed triggering the PMTs with low light level (SPE) at a rate of 100 Hz. First, the recovery time is studied after gain vs HV measurements, although the average number of p.e. is lower than 1, at the maximum voltage (1900 V) the output current is high enough to reduce the effective PMT gain at CT as it is shown in Fig. 10(a). For the PMT shown, after measurements at 1900 V, the gain value obtained at 1400 V drops a 30% with respect to the initial measured gain and the gain recovery requires about a day on average. After the linearity measurements where PMTs are exposed to light levels of ~ 1000 p.e. at 10^8 gain, a similar behavior is observed, see Fig. 10(b). Finally, a more permanent effect over the gain is caused by high rate signals of the order of MHz, as can be observed in Fig. 10(c). In this case, the gain decreases by a factor of 2. For some PMTs, a week after illuminating them with high frequency signals, the gain is still a 40% lower than the nominal gain. However, other PMTs recover faster (in 3 days). In any case, the recovery time varies a lot from one PMT to another. The theoretical value of the PMT maximum output current during the previous test is calculated to verify that the gain recovery time depends on it. The PMT maximum output current is calculated as $I_{out} = e^- \cdot G \cdot npe \cdot f$ where e^- is the electron charge, G is the PMT gain, npe is the average number of p.e. during the test, and f the light pulse rate in Hz. The results are a few μA for the Gain vs V and linearity tests, and hundreds of μA for the light rate test.

4.3 Linearity

The PMT response is studied as a function of the light intensity. The amount of scintillation light arriving to the PMTs in ProtoDUNE-DP will vary from a few p.e. to thousands of p.e. depending on the particle track energy and distance to the PMTs. Thus, the response of the PMTs should be linear in a wide dynamic range. The PMT base was designed to fulfill this goal, and the deviation of the linear response is primarily caused by the anode saturation.

The PMT linearity is studied at gains up to 10^8 using a set of 11 filters with different attenuation factors connected to the light source through optical fibers. To avoid the fatigue effect, explained in section 4.2, measurements are done from low light (SPE) to high light levels (up to 1000 p.e.). The expected amount of light is estimated relatively to the measured one in the linear region, taking three reference filters and considering their transmission factor. As known from previous tests, the PMT response is linear up to at least 100 p.e. for gain $\sim 10^7$ and up to 40 p.e. for gain $\sim 10^8$. For low intensity illumination (SPE regime) the average number of p.e. is obtained from the fit of the SPE spectrum, but it is not used as reference due to its large uncertainty. The 405 nm laser (<1ns pulse) and the 460 nm LED (40 ns pulse) are used to check the effect of the pulse profile on the anode saturation. For the same amount of detected light, the shorter the light pulse, the higher output peak current leading easier the PMT to saturation due to space-charge effects on the last dynodes.

4.4 Light rate

In ProtoDUNE-DP, a continuous background of light pulses is expected due to the secondary scintillation light produced on the gaseous phase of the argon by the drifted electrons. To study how this can affect the PMT performance, dedicated tests are carried out. In these tests, the light

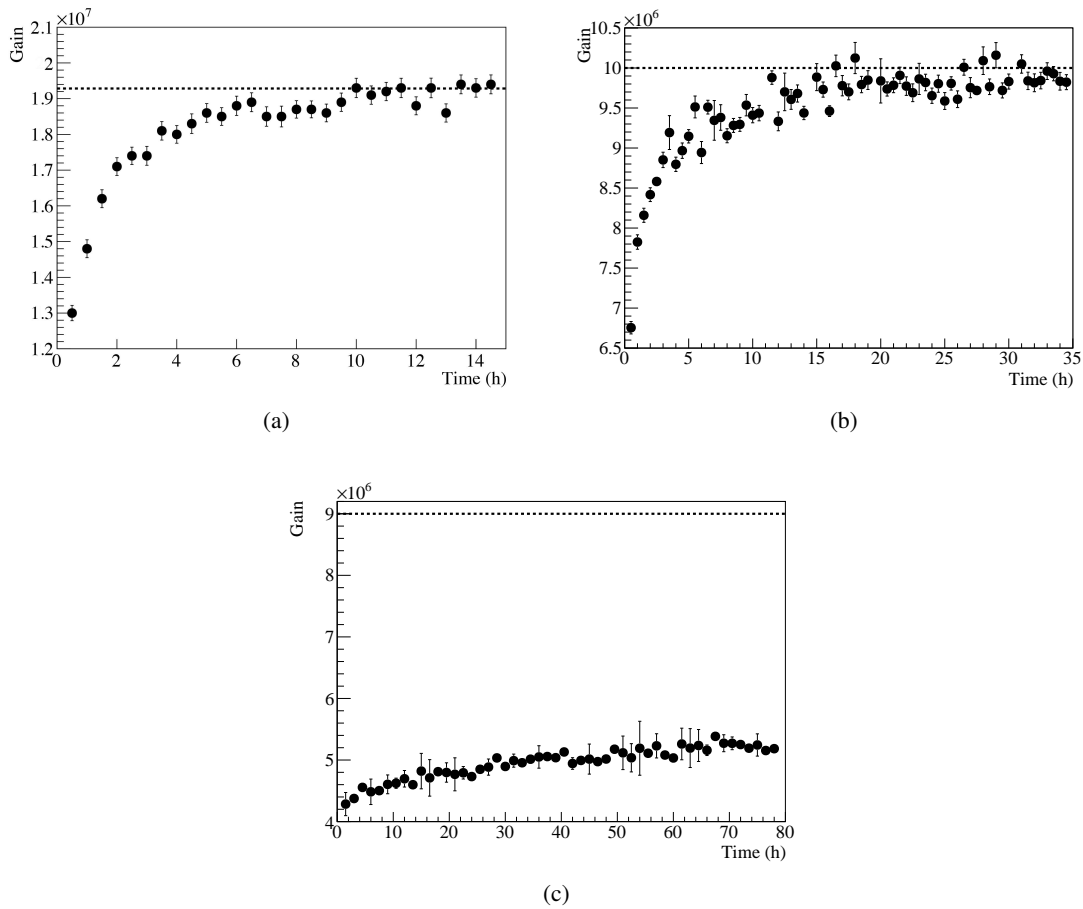


Figure 10. (a) Gain evolution after raising the voltage from 1400 V to 1900 V and back to 1400 V. (b) Gain recovery time, after linearity measurements. (c) Gain recovery time, after high rate measurements. The dotted lines represent the expected gain without the fatigue effect.

intensity is set to different levels, from few p.e. to 150 p.e., using the set of filters. For each light level, the light pulses emission frequency is swept from low (100 Hz) to high frequencies (10 MHz). The tests are carried out with the laser and the LED to check the effect of the pulse profile. For each combination of light level and pulsed frequency, the charge spectra of the PMT is obtained to calculate the averaged amount of light observed by the PMT.

Increasing the rate of the light pulses produces a proportional increase of the average output current. As the base design is based on resistors, the PMT inter-dynode voltages have a dependency with the PMT output current making the PMT response not linear when the light rate increases over a certain limit. The current through the base resistors has two components: the polarization current, constant and provided by the power supply, and the PMT output current that goes through the resistors in the opposite direction. As the total voltage applied to the base is kept constant by the power supply, a decrease on the last dynodes voltage (by the increase of the output current), makes higher the voltage on the first dynodes increasing the PMT gain. If the voltage on last dynodes continues decreasing (by the increase of the output current) at some point this voltage

is not enough to maintain the current flow to the anode, and it decreases following the typical I-V curve of a vacuum diode [17]. The only difference is that in the vacuum diode, the cloud of electrons is generated by a filament while in the PMT it is generated by the incident light and the previous dynodes. Besides that, the PMT output current does not depend any more on the light input intensity, only on the light rate that is changing the voltage on the last dynodes.

Then, the expected PMT response vs. light rate can be divided in three zones: first, the linear response, from <1 Hz; second, the over-linearity region, where the PMT gain increases; and third, the saturation region, when the voltage between the last dynode and the anode is close to zero and the PMT output decreases with the light rate. The PMT output is never zero because the initial velocity of the p.e. is not zero, therefore some of them can be collected by the last dynode even if the potential difference between the cathode and the first dynode is zero. To reach the zero output this potential should be negative.

At CT, the fatigue effect observed on the PMT gain (as explained in section 4.2), compensates the beginning of the gain increase with the light rate leading to a small reduction of the over-linearity region.

5 PMT validation results

Although these PMTs are designed to operate at CT, the manufacturer does not provide information about the CT behavior. Then, to validate the PMT model selection, different tests were carried out to several PMTs at RT and CT, and the results are presented in this section.

5.1 Dark Current

The DC rate as a function of the HV is measured. Figure 11 shows a typical plot of the DC at RT and CT. The plot is done as a function of the gain to equalize the response at RT and CT, as expected. In general, the DC at CT is higher than at RT for the same gain. For this particular PMT, the DC increases from 0.6 kHz at RT to 1.9 kHz at CT for a gain of $1.5 \cdot 10^7$, being the behavior of this PMT representative of other PMTs.

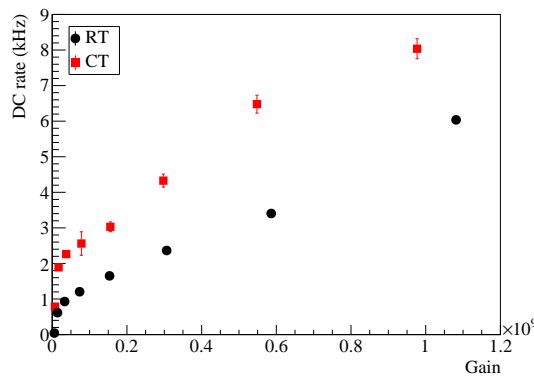


Figure 11. DC vs gain at RT and CT for one PMT. For each gain, DC is measured every 10 s during 5 min, the average value is plotted and the error bars represent the rms.

5.2 Gain

Gain calibration curves at RT and CT (at 77 K) are measured, and the result for one PMT can be seen in Figure 12. The slope of the curves follows a simple power law. For the same HV, the gain at CT is lower than at RT. Being the gain 10^7 at RT, it decreases a 76% due to cryogenic conditions. With an increase of 170 V, the previous gain can be achieved for this PMT.

The gain is also measured at a temperature closer to the one in ProtoDUNE-DP, which will be 94 K, taking into account the pressure at the bottom of the LAr cryostat. To achieve a higher temperature, an over-pressure of 1 bar is applied to the vessel, which is the maximum allowed by the set-up. While the temperature with LN₂ at atmospheric pressure is 77 K, during these tests 83 K are reached. Gain variations are found (see Figure 12), compatible with expectations [11]. For the same PMT, a 10^7 gain at RT decreases a 66% at 83 K. This means that 130 V more than at RT are required to obtain the same gain. In total, 4 PMTs were measured at 83 K, and the gain decreases on average a $60 \pm 9\%$.

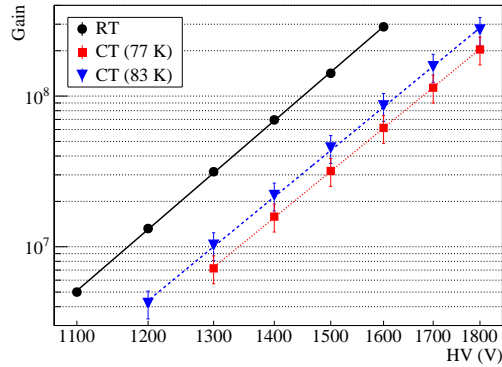


Figure 12. Gain vs HV at RT, at two CT (77 K and 83 K) for the same PMT. The dots represent the measurements, and the lines the fit explained in section 4.2. The vertical error bars correspond to the average variation in the gain obtained from repeated measurements: a 7% at RT and a 21% at CT.

5.3 Linearity

The response of several PMTs as a function of the light intensity is measured at RT and CT. The response at RT for $\sim 10^7$ and $\sim 10^8$ gains illuminating a PMT with the laser is shown in Figure 13. For gains $< 10^6$ the response has been observed to be linear in the tested range (up to ~ 1000 p.e.). For gains close to 10^7 , the PMT remains linear up to 200 p.e., while for larger gains ($> 10^8$) the PMT response deviates from linearity with only 75 p.e., and a saturation regime is reached. Same response is observed for all tested PMTs, as an example the perfect agreement of three PMTs is shown in Figure 13. The uncertainty in the measured number of p.e. is a 4% and comes from the gain variation obtained fitting spectra at different light levels. On the other hand, the error in the expected number of p.e. is a 9% and corresponds to error propagation of the uncertainties in the gain estimation and in the measurement of the transmission of the filters.

The PMTs are also illuminated with the LED, and the results are compared to the laser ones in Fig. 14(a). The linearity range increases when the light source is wider, showing a clear dependency

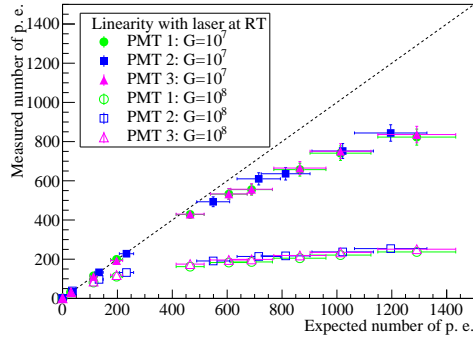


Figure 13. Measured vs expected number of p.e illuminating three PMTs at different gains RT with the laser.

with the pulse shape in the PMT saturation. The LED provides a light source closer to the expected one in ProtoDUNE-DP since the S1 fast component of the scintillation light is ~ 6 ns. At CT, the PMT response is just slightly worse than at RT when the PMT is illuminated by the laser. For instance, for a 10^8 gain and 500 p.e., the measured number of p.e. is a 60% and a 70% lower than expected at RT and CT, respectively. However, as can be seen in Fig. 14(b), the linear range when the PMT is illuminated by the LED at CT is shorter than at RT, and similar to the laser at CT. Therefore, despite the very good linearity at RT, the PMT response is saturated at 300 p.e. for a gain of 10^7 at CT.

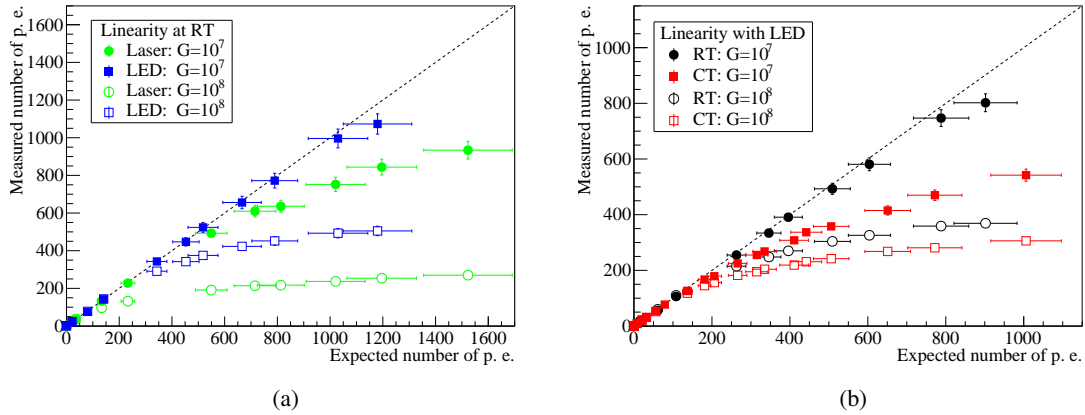


Figure 14. Comparison of the measured vs expected number of p.e. illuminating the PMT with the LED and the laser at RT (a) and comparison of RT and CT for the LED (b).

5.4 Light rate

The PMT response is studied for pulsed frequencies from 100 Hz to 10 MHz using the laser and the LED as light sources and different light intensities.

At RT, see Figure 15(a), the three regions explained in section 4.4 are observed: the PMT response is flat until a given frequency (>10 kHz) which depends on the charge; then, the overlinearity effect is observed; and the PMT saturation (>500 kHz). At CT, the PMT response is

expected to be the same as at RT, see Figure 15(a), as the saturation curve depends only on the base design. The expected PMT gain reduction, as the average output current increases (see section 4.2), compensates and reduces the over-linearity region. The same result is observed for different PMTs, see Figure 15(b).

The frequency sweep is also done using the LED, and the results, shown in Figure 16, suggest that the response is very similar, but the over-linearity starts at slightly higher frequencies when the LED is used. As the LED light pulses are wider, the PMT output peak current is smaller (for the same charge) moving the over-linearity effect to higher frequencies. For low intensity signals, as expected for the S2 light in ProtoDUNE-DP, the PMT response is linear until ~ 1 MHz, far enough for our purpose.

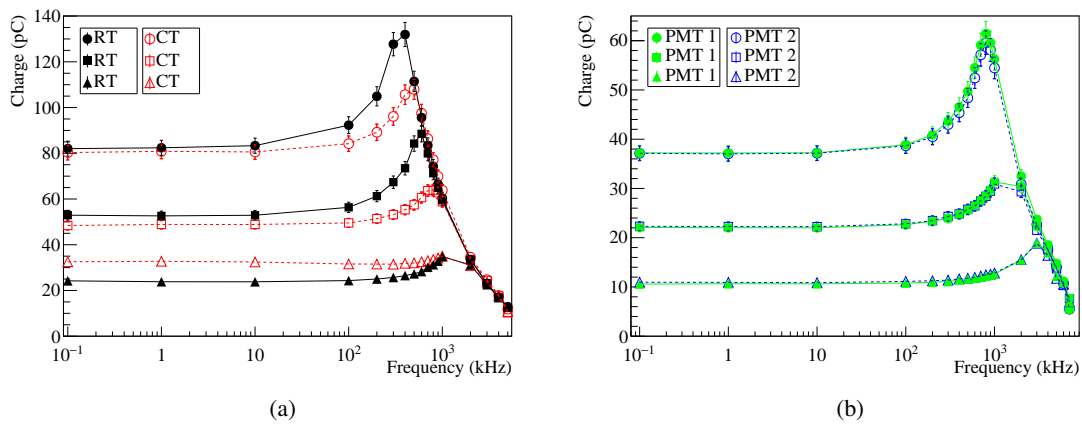


Figure 15. (a) PMT LED frequency response at RT and CT for different amounts of light. (b) Two PMTs frequency response comparison for laser at RT. The vertical error bars are a 4% and are given by the variation of the charge obtained when repeating the measurements.

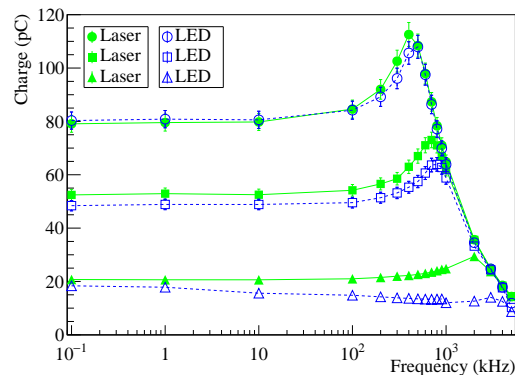


Figure 16. Charge vs frequency for LED and laser with similar charge at CT. The vertical error bars are a 4% and are given by the variation of the charge obtained when repeating the measurements.

5.5 PMT base validation

In order to validate the design of the PMT base, it is tested at RT and CT in terms of gain, dark rate, and linearity. As expected, the PMT gain with both configurations, PB and NB, is similar. In order to compare DC rate vs voltage dependence, both bases are tested on the same PMT and on the same darkness conditions. The results show that the behavior of both bases is similar at voltages up to 1600 V, and at higher HV the DC rate increases more on the NB reaching a rate around 50% higher than the PB at 1900 V. The base with negative power supply shows higher dark rate than the positive one because the photo-cathode is at high voltage and spurious pulses could appear due to current leakage through the glass or due to electro-luminescence in the glass.

For the linearity response, the positive base shows slightly better results, see Figure 17(a). On the positive bias base, the power supply filter capacitor is closer to the anode which increases the charge reservoir for the PMT output increasing slightly the linearity range.

For the study of the response with the light rate, the tests are done following the procedure described in section 4.4. The positive circuit shows also better results, as shown in Figure 17(b). The difference between the two bases is also due to the different position of the filtering capacitor on the base. To verify it, a PB without this capacitor was also tested and its behavior was slightly worse than with the NB, see Figure 17(b), making clear that the presence of this capacitor close to the anode improves the linearity of the PMT. Increasing the capacity of this capacitor did not improve the response any further at the tested light levels. These tests confirm the better performance of the PB.

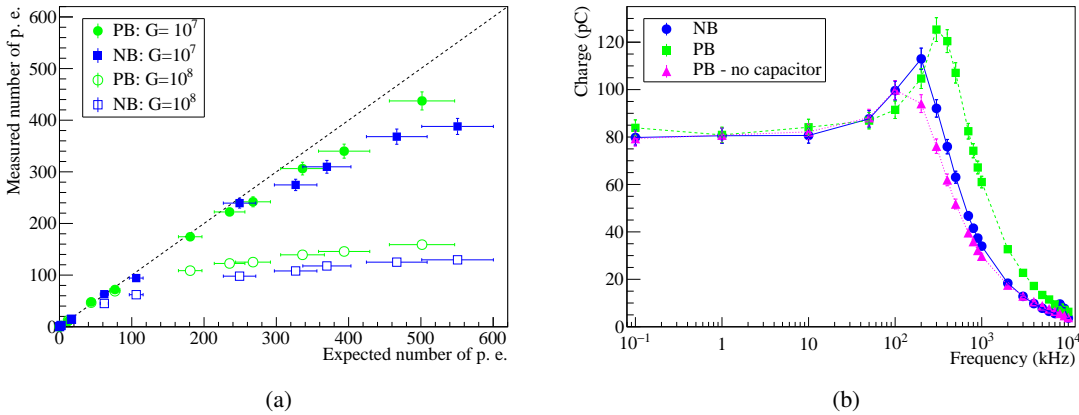


Figure 17. (a) Measured vs expected number of p.e. for the NB and PB at RT with the laser. (b) Response vs light rate for NB, PB and PB without filtering capacitor at RT with the laser.

6 ProtoDUNE-DP PMT characterization

Last, all the PMTs to be installed at ProtoDUNE-DP are characterized. Measurements with 40 (36 + 4 spares) PMTs are taken to verify the successful functioning and create a database to be used during the detector commissioning and operation. DC and gain as a function of HV at RT and CT are measured. Also, typical waveforms for all the PMTs at 10^7 gain are recorded.

6.1 Dark Current

The DC rate is measured for the 40 PMTs at several HVs as explained in section 4.1. In particular, the DC rate at 10^9 gain is measured to compare with the value given by the manufacturer. Figure 18(a) shows the correlation between the rates measured at CIEMAT (at the HV specified by the manufacturer) and the ones provided by Hamamatsu at RT. In general, similar results are obtained. However, two of them had to be replaced, as one had no signal and another one showed a DC rate of around 100 kHz (almost 60 times the expected rate from Hamamatsu). It is worth noting that the defective PMTs are not shown in the plot, but the replacements are shown instead.

On average, as shown in Figure 18(b), DC rate is 0.4 ± 0.2 kHz when the PMTs operate at $\sim 10^7$ gain at RT, and DC rate is always below 1.4 kHz. However, at CT, DC rate increases up to 1.7 ± 0.3 kHz, and some PMTs reach up to 2.5 kHz. The PMTs with very unstable DC rates in time (i.e. large error bars in the Fig. 18(a)) were inspected by Hamamatsu and although no defects were found, they can be designated as spares. Also, the PMTs with the highest DC rate are candidates to be spare ones.

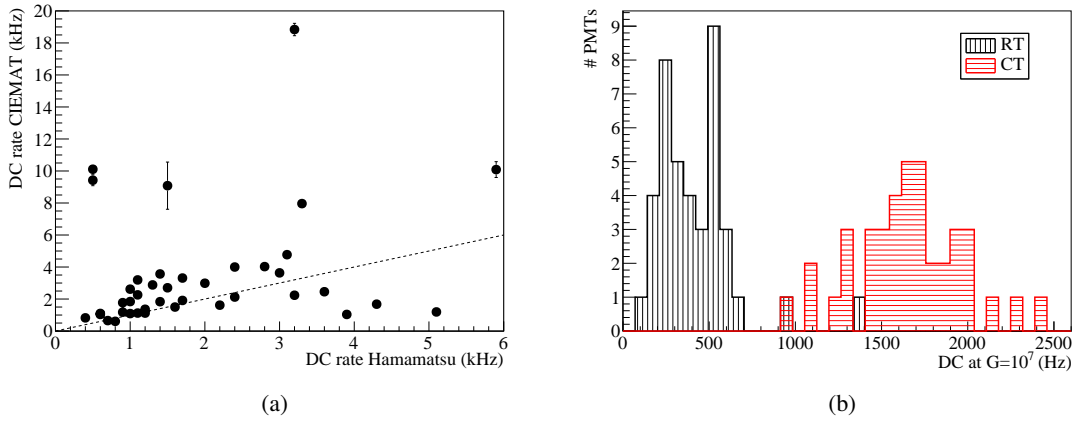


Figure 18. (a) DC measured at CIEMAT vs Hamamatsu for 10^9 gain for the 40 PMTs. DC is measured every 10 s during 5 min, and the error bars represent the rms of the average value. The dotted line represents the identity line. (b) DC histograms for 10^7 gain at RT y CT measured at CIEMAT for the 40 PMTs. At RT, DC rate is on average 0.4 ± 0.2 kHz, and at CT, 1.7 ± 0.3 kHz.

6.2 Gain

The gain results from the characterization of the 40 PMTs are presented here. Figure 19 shows the correlation between the HV determined at CIEMAT for a 10^9 gain, and the HV required according to manufacturer specifications (both values at RT). The CIEMAT HV is extrapolated from the gain calibration curve of each PMT. A good correlation is observed with only a 2.3% deviation. In Figure 20, the HV required for a 10^7 gain at RT and CT is presented. Higher HV, 170 ± 72 V on average, needs to be applied at CT to reach the same gain, which is equivalent to a $71 \pm 14\%$ gain drop at CT.

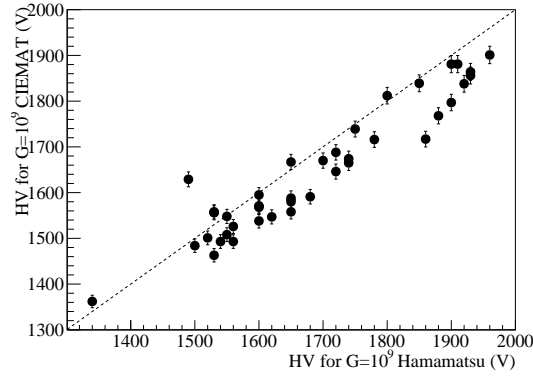


Figure 19. HV applied at CIEMAT compared to the HV provided by Hamamatsu for 10^9 gain for the 40 PMTs. The dotted line represents the identity line.

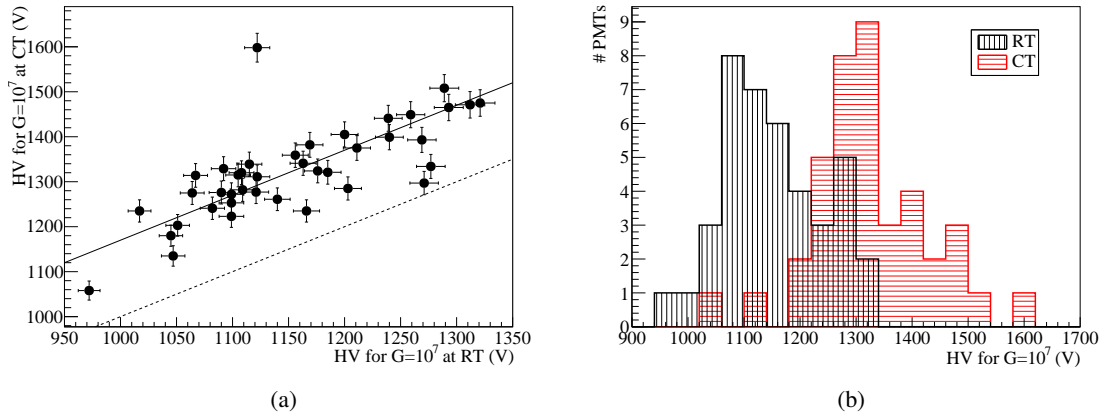


Figure 20. (a) HV at RT vs CT for 10^7 gain measured at CIEMAT for the 40 PMTs. The dotted line represents the identity line and the solid line the identity line shifted 170 V. (b) Histogram of HV required to obtain a 10^7 gain at RT and CT. The average HV is 1154 ± 87 V at RT, and 1324 ± 103 V at CT.

Conclusions

The ProtoDUNE-DP experiment aims to build and operate a LAr TPC detector at CERN to fully demonstrate the dual-phase technology at large scale for DUNE, the next generation long-baseline neutrino experiment. The photon detection system will add precise timing capabilities, and will be formed by 8-inch cryogenic photomultipliers from Hamamatsu positioned at the bottom of the detector. The validation measurements of the PMT model (R5912-20Mod) and the base design at cryogenic temperature are described. In addition, the 40 PMTs to be used in ProtoDUNE-DP are characterized to ensure their performance according to the specifications and valuable results to be used by other experiments are obtained.

It is observed that the dark current rate at CT is higher than at RT due to non-thermal contributions, i.e. at a gain of 10^7 the DC rate is on average to 1.7 ± 0.3 kHz at CT while at RT is 0.4 ± 0.2 kHz. This effect has been observed previously in different PMTs models, being

proportional to the photo-cathode area [13]. From RT to CT, the gain decreases, and a gain of 10^7 at RT, drops a $71 \pm 14\%$ when the PMT operates at 77 K, and a $60 \pm 9\%$ at 83 K.

At CT, a fatigue effect is observed as the PMT output current increases, either, due to high gain, high light intensity or high light rate. The gain recovery time depends on the PMT excitation (output current) and varies from PMT to PMT. The largest effect is observed when the excitation comes from high frequency signals of \sim MHz.

The linearity of the PMT response with the incident light depends on the PMT gain and the width of the incident light pulses. For fast signals (< 1 ns pulse) the PMT remains linear up to at least 1000 p.e. for a 10^6 gain, but losses linearity at 75 p.e. in the case of 10^8 gain. However, when the same amount of light is distributed on a wider (40 ns) pulse, the linearity region of the PMT increases. A slightly worse behavior is observed at CT for the laser, but an earlier saturation is observed for the LED in comparison to RT.

PMT response with the light rate is flat until > 10 kHz for less than 100 p.e.. At CT, the PMT response is expected to be the same as at RT, as the saturation curve depends only on the base design, but gain reduction compensates and reduces the over-linearity region.

For these reasons, characterization tests at CT before installing the PMTs are required, and a dedicated photon calibration system is recommended to monitor the PMT during the experiment data taking period. It is concluded that these PMTs are validated and will be used in ProtoDUNE-DP.

Acknowledgments

This project has received funding from the European Unions Horizon 2020 Research and Innovation programme under Grant Agreement no. 654168 and from the Spanish Ministerio de Economía y Competitividad (SEIDI-MINECO) under Grants no. FPA2016-77347-C2-1-P, FPA2016-77347-C2-2-P, MdM-2015-0509, and SEV-2016-0588.

References

- [1] R. Acciarri et al., *Long-Baseline Neutrino Facility (LBNF) and Deep Underground Neutrino Experiment (DUNE) Conceptual Design Report Volume 2: The Physics Program for DUNE and LBNF*, [arXiv:1512.06148](https://arxiv.org/abs/1512.06148).
- [2] R. Acciarri et al., *Long-Baseline Neutrino Facility (LBNF) and Deep Underground Neutrino Experiment (DUNE) Conceptual Design Report Volume 4: The DUNE detectors at LBNF*, [arXiv:1601.02984](https://arxiv.org/abs/1601.02984).
- [3] L. Manenti, *ProtoDUNEs, Proceedings of Prospects in Neutrino Physics (NuPhys2016)* (2017), [[arXiv:1705.05669](https://arxiv.org/abs/1705.05669)].
- [4] L. Agostino et al., *LBNO-DEMO: Large-scale neutrino detector demonstrators for phased performance assesment in view of a long-baseline oscillation experiment*, CERN-SPSC-2014-013, SPSC-TDR-004, [arXiv:1409.4405](https://arxiv.org/abs/1409.4405).
- [5] C. Cuesta et al., *Photon detection system for ProtoDUNE dual phase*, *JINST* **12** (2017) C12048.
- [6] Hamamatsu. <http://www.hamamatsu.com>.
- [7] T. Briese et al., *Testing of Cryogenic Photomultiplier Tubes for the MicroBooNE experiment*, *JINST* **8** (2013) T07005.

- [8] T. Caldwell et al., *Characterization of the R5912-02 MOD photomultiplier tube at cryogenic temperatures*, *JINST* **8** (2013) C09004.
- [9] A. Badertscher et al., *ArDM: first results from underground commissioning*, *JINST* **8** (2013) C09005.
- [10] G. Raselli et al., *Test and characterization of 20 pre-series hamamatsu R5916-MOD photomultiplier tubes for the ICARUS T600 detector*, *IEEE Nuclear Science Symposium, Medical Imaging Conference and Room-Temperature Semiconductor Detector Workshop* (2016) 1–5.
- [11] J. Nikkel et al., *Demonstration of photomultiplier tube operation at 29 K*, *JINST* **2** (2007) P11004.
- [12] Hamamatsu, “PMT handbook, third edition.”
https://www.hamamatsu.com/resources/pdf/etd/PMT_handbook_v3aE.pdf, 2007.
- [13] H. Meyer, *Dark Rate of a Photomultiplier at Cryogenic Temperatures*, [arXiv:0805.0771](https://arxiv.org/abs/0805.0771).
- [14] H. Meyer, *Spontaneous electron emission from a cold surface*, *EPL* **89** (2010) 58001.
- [15] E. Bellamy et al., *Absolute calibration and monitoring of a spectrometric channel using a photomultiplier*, *NIM A* **339** (1994) 468.
- [16] W. A. Rosen and F. R. Chromey, *The implications of photomultiplier fatigue for pulse-sounding photometry*, *The Astronomical Journal* **90** (1984) 139.
- [17] P. series of publications, “Laboratory Experiments.”
http://educyclopedia.karadimov.info/library/4_1_10.pdf, 2008.